OPTION PRICING UNDER STOCHASTIC VOLATILITY OF US REITS

1 author:

Gianluca Marcato
Henley Business School (University of Reading)
58 PUBLICATIONS **500** CITATIONS

Option pricing under stochastic volatility

A numerical investigation of the Heston model

Rickard Kjellin Gustav Lövgren

January 25, 2006

Abstract This thesis investigates pricing of options in a world beyond Black-Scholes. Primarily the Heston stochastic volatility model is examined. This model is calibrated to S&P500 market data. With the obtained parameters as a starting point, we investigate the properties of the model and the behavior of option prices in the Heston framework.

When pricing European call options using Monte Carlo, our results indicate that the Monte Carlo pricing puts a downward bias on the option price, compared to the closed form price.

In an attempt to price American call options in the Heston model, a finite difference scheme as well as a lattice approach was tested using standard numerical methods. Several problems and instabilities were encountered, suggesting that more advanced numerical schemes are needed.

Some exotic options (barrier, lookback and Asian) were priced using a Monte Carlo approach. The prices produced seemed to converge quite well. However, the downward bias on the Monte Carlo prices of European call price casts doubt on the Monte Carlo price of the more exotic options as well.

For all options investigated, a sensitivity analysis with respect to parameters have also been performed. Noteworthy is that the correlation between the volatility and the stock price affects the behavior of option prices quite much.

Acknowledgments The authors would like to thank Alexander Herbertsson at the Centre for Finance for all the help and assistance provided in the making of this thesis.

Contents

Chapter 1

Introduction

1.1 Introduction

In this paper we will look at option pricing in a more general setting than in the Black-Scholes framework. We will especially look closer at the model suggested by Heston. The model is a stochastic volatility model, meaning that we do not only let the stock price vary randomly, but also let the the volatility of these random fluctuations be random. We will investigate if this model can better reflect the market than the Black-Scholes model. We will also assess how practically implementable this model is and try to draw conclusions on how options behave in a Heston framework.

The paper is arranged in four chapters. In Chapter one, we go through some of the foundations of derivatives and derivatives pricing. This includes a reminder of some types of options, vanillas as well as some more exotic, and a short introduction to the Black-Scholes model and its limitations. With this as the starting point, we will then present some other models that have been suggested throughout the years. These models in general have some feature/features supported by the real world (i.e. the market), but are also often more mathematically complex than the Black-Scholes model. The chapter will then be ended by a introduction to some of the methods and tools used in derivatives pricing. This includes, for example, the concept of risk neutrality and Monte Carlo pricing. It also includes a discussion of the means by which one can calibrate ones model to the real world.

In Chapter two, we look closer at the Heston stochastic volatility model. This model is one of the most popular stochastic volatility models. This is probably much due to the face that a closed form solution to the price of a European call option can be derived. This formula will be presented, and we will also show that the model can reproduce the so call implied volatility smile, a market feature that will be described in Chapter one. We will also

look at, and give a description of, the parameters of the model.

In Chapter three, we will calibrate the Heston model to actual market data. Using the parameters obtained from this calibration, we will then price some different types of options, using various numerical methods. This includes Monte Carlo, pricing using finite difference approximation of the partial differential equation governing the option price, as well as pricing using lattice methods. We will also look at the sensitivity of the options prices with respect to the parameters. For the European call option, a closed form of the Delta and Gamma will be derived. The chapter will be ended by a discussion of the obtained results.

The ending chapter contains a summary of the conclusions and a discussion of the obtained results.

1.2 Derivatives

Derivative contracts are securities whose value are contingent on some other financial instrument or variable, called the underlier. The derivatives that will be discussed in this paper will all have a stock or a stock index as the underlier, however markets exist in a wide variety of derivatives. Examples are energy and commodity derivatives, weather derivatives etc. Yet another example is the credit derivative market, which has grown tremendously in recent years.
The payoff from a derivative can be written as a functional of the underlying asset price process. Let $(S_t)_{t\geq 0}$ be the asset price path. We distinguish between European style of derivatives, where the payoff is calculated at the date of maturity,

$$\begin{aligned} V_T^{European} &= \xi(\{S\}_\tau), \\ \tau &= [0, T], \end{aligned} \tag{1.1}$$

and American derivatives, where the holder may chose a premature exercise date.

$$\begin{aligned} V_{\widetilde{t}}^{American} &= \xi(\{S\}_{\widetilde{\tau}}), \\ \widetilde{\tau} &= [0, \widetilde{t}], \\ \widetilde{t} &\in [0, T] \end{aligned} \tag{1.2}$$

Here follows a presentation of various derivatives that will be addressed later in the thesis.

1.2.1 Options

Options are derivative contract were the holder may chose to forfeit the contract. She has the right to exercise, but not the obligation.

Call options A call option on an underlying asset gives the holder the right to buy the asset at a predetermined price – the *strike price* – at a specified time in the future. For a European option, this time point is fixed at the maturity time. The American option allows the holder to buy the asset for the strike price at any time up to the maturity date. The payoff function looks like[1] $V(t) = (S_t - K)^+$, if K denotes the strike price and S_t is the spot price of the underlying asset at the exercise date.

Put options The put works in the opposite way of the call, allowing the holder to sell the underlying asset at the strike price. The payoff is $(K - S_t)^+$.

Digital options The digital, or binary option pays out a unit amount on the maturity date if the spot of the underlying asset is above some predetermined boundary. The payoff function is $V(t) = \mathbf{1}_{\{S_t \geq B\}}$, where $\mathbf{1}_{\{A\}}$ is the indicator function, which takes value 1 if the event A occurs, and 0 otherwise.

The options discussed so far have been *simple*, in that the payoff function only takes the spot price of the underlying as argument. The class of lookback options are path-dependent and instead of a simple function, the payoffs are functionals of the spot price trajectory. In theory, the contracts often require continuous monitoring of the paths, while in reality this is not possible. We will adress this issue later in the thesis.

Barrier options The barrier options toggle payoff on or off when the underlying hits a barrier. One example is the *down-and-out* digital option. If the underlying spot price hits or crosses a predetermined boundary B up to the maturity date, the option pays out 0. It the spot price trajectory stays above the boundary during the whole time interval the option pays out 1. Formally we have, $V(t) = \mathbf{1}_{\left\{ \inf\limits_{t^* \in [0,t]} S_{t^*} > B \right\}}$.

Similar to the down-and-out is the *up-and-out* digital option. It's payoff is instead 1 if the stock price stays below an upper bound, and 0 if the stock price hits or crosses the upper bound.

The barrier options mentioned so far are digital, i.e. they pay either zero or one. A barrier options can have other types of payoffs. A

[1] We use the convention that $(x)^+ = \max(x, 0)$

European up-and-out call option for example pays of like a standard European call option, assuming that the stock price stays below the boundary. Otherwise it pays of zero.

Lookback options One of the more common lookback options is the maximum-to-date call. It is almost like a European call, but instead of using the spot price of the underlying asset for exercise, the strike is compared to the maximum of the asset price path up to the date of exercise. A *maximum-to-date* call has a payoff function of the form $V(t) = \max(\sup_{t*\in[0,t]} S_{t*})$.

Arithmetic Asian option The Asian options uses the mean level of the spot price process for comparison. The arithmetic Asian call option uses the ordinary arithmetic mean, $\hat{x}(t) = \frac{1}{t-a}\int_a^t x(s)ds$, and has the following payout function, $V(t) = (\frac{1}{t-a}\int_a^t S(s)ds - K)^+$ and a denotes the point in time from where the mean is taken.

To obtain the option the holder must pay the issuer of the derivative a fee, denoted the *premium*. The premium is a theoretical construction, derived by using arbitrage arguments, a concept discussed below.

1.2.2 Arbitrage

Central to the development of the field of modern finance is arbitrage. An arbitrage is essentially the possibility to make money out of nothing. In a simple two-period setting, an arbitrage is a portfolio strategy such that the value of the portfolio at time 0 is zero, $V_0 = 0$, and at time 1 the value V_1 of the portfolio satisfies $\mathbb{P}\{V_1 \geq 0\} = 1$ and $\mathbb{P}\{V_1 > 0\} > 0$; that is, there is a nonzero probability of making a profit and zero probability of making a loss.

1.2.3 Replicating portfolios

In order to justify a fair price to a derivative, ϕ, the standard way to proceed is to find a portfolio $\Pi(t)$, of tradeable assets whose cash flows exactly replicates the cash flows of the derivative. Then at any time t, in order to rule out the possibility of arbitrage, the price of the derivative, $V_\phi(t)$, must be equal to the value of the replicating portfolio, $V_\Pi(t)$.

If the derivative costs less than its replicating portfolio, an arbitrage strategy would be to form a new portfolio, $\Psi(t)$, consisting in a long position in the derivative contract and a short position in the replicating portfolio, $\Psi(t) = \{\phi, -\Pi\}$. Since the cash flows from the two components of the portfolio exactly offset each other, the agent will make a profit of $V_\phi(0) - V_\Pi(0) > 0$ almost surely. In the opposite case, where the derivative contract is more

expensive than its replicing portfolio, the portfolio $\widetilde{\Psi}(t) = \{-\phi, \Pi\}$ is an arbitrage strategy.

Hence, if we may construct a replicating portfolio for the contract, we can deduce a fair value of the derivative that, in view of arbitrage arguments, must be the right price.

1.3 Black Scholes

In 1973 Black and Scholes (BS) [3] suggested the following stochastic differential equation (SDE) as a model for the dynamics of a stock price process:

$$dS_t = \mu S_t dt + \sigma S_t dW_t \tag{1.3}$$

where S_t is the stock price at time t, μ is the return on the stock and σ the volatility of the stock, defined as the standard deviation of the logreturns and W_t is a standard Browian motion. The first term of the right hand side is called the drift. It is the deterministic part of the equation, and contributes to driving the process value S_t in a deterministic way. The second part, called the diffusion, is the stochastic part. It adds a random noise to S_t. This random noise is amplified by the volatility σ.
The BS model is complete[2], i.e. we can apply simple arbitrage arguments to get a derivative pricing formula. Solving Equation (1.3) yields the solution:

$$S_t = S_0 e^{\left(\mu - \frac{1}{2}\sigma^2\right)t + \sigma W_t}$$

which is sometimes called a geometric Brownian motion. The stock price is in this model log-normally distributed.
Applying arbitrage arguments to the BS model will result in a partial differential equation (PDE) governing the option price. This PDE can then be solved for different pay-off functions. For a European call option, the option price C_{BS} will be given by the following closed form formula:

$$C_{BS}(t, S_t, K, T, \sigma_I, r) = S_t N(d_1) - K e^{-r(T-t)} N(d_2) \tag{1.4}$$

where

$$d_1 = \frac{\ln\left(\frac{S_t}{K}\right) + \left(r + \frac{\sigma^2}{2}\right)(T-t)}{\sigma\sqrt{T-t}}$$
$$d_2 = d_1 - \sigma\sqrt{T-t}$$

and t is the current time, T the time of maturity, S_t the current stock price, r the risk free interest rate, K the strike price and $N(x) = \int_{-\infty}^{x} \frac{1}{\sqrt{2\pi}} e^{\frac{-t^2}{2}} dt$ is the cumulative distribution formula for a normal random variable with mean 0 and variance 1.

[2] A complete market is one in which all cashflows can be replicated by S_t and the riskfree bond.

1.3.1 The Greeks

The sensitivity of an options price with respect to a variable is commonly referred to as a *Greek*. The name stems from the fact that these quantities usually are denoted by Greek letters.

Delta, Δ measures the sensitivity of the option price with respect to the current stock price S_0, i.e. $\Delta = \frac{\partial C}{\partial S_0}$, where C denotes the option price. In the Black-Scholes model, the Delta of a European call option can be shown to be

$$\Delta_{BS} = N(d_1)$$

using the notation from Equation (1.4).

Gamma, Γ measures the sensitivity of the delta with respect to the current stock price. It is the second derivative of C with respect to S_0, $\Gamma = \frac{\partial^2 C}{\partial S_0^2}$. In the Black-Scholes model, the gamma equals

$$\Gamma_{BS} = \frac{\varphi(d_1)}{S_0 \sigma \sqrt{T-t}}$$

where $\varphi(x)$ is the density function for a normal variable with mean 0 and variance 1.

Kappa, K is the sensitivity of the option price with respect to the volatility σ, i.e. $\mathrm{K} = \frac{\partial C}{\partial \sigma}$. It is sometimes refered to as *vega*.

Theta, Θ measures the effect of time on the price of an option, i.e. $\Theta = \frac{\partial C}{\partial t}$.

1.3.2 Limitations

The BS model contain some rather strong simplifications of the real world. Among them:

- The model implies that the log-returns are normally distributed. Empirical studies of actual market data have suggested that this is often not the case. We will return to this below.
- It is a continuous model. Trading, however, takes place in discrete time intervals.
- The model assumes zero transaction costs. Since the option prices are derived by means of creating a replicating portfolio which will be continuously rebalanced, this is a rather important point to make. Replicating continuously would, in theory, yield infinitely large losses.
- The volatility is assumed to be known and constant over time. This assumption has been relaxed by a number of authors, and in this paper we will look at some of these models.

Normality

As mentioned above the BS model implied that the log-returns are normally distributed. However, historical returns often displays non-normal features. The tails of the distribution are fatter than the tails of a normal. This means that large moves (both up and down) happens more often than suggested by the model. The empirical disribution is also commonly peaked around the center. Figure 1.1 shows the distribution of the S&P500 daily log-returns on the time period 2-Jan 1998 to 31-dec 2004 along with the fitted normal distribution.

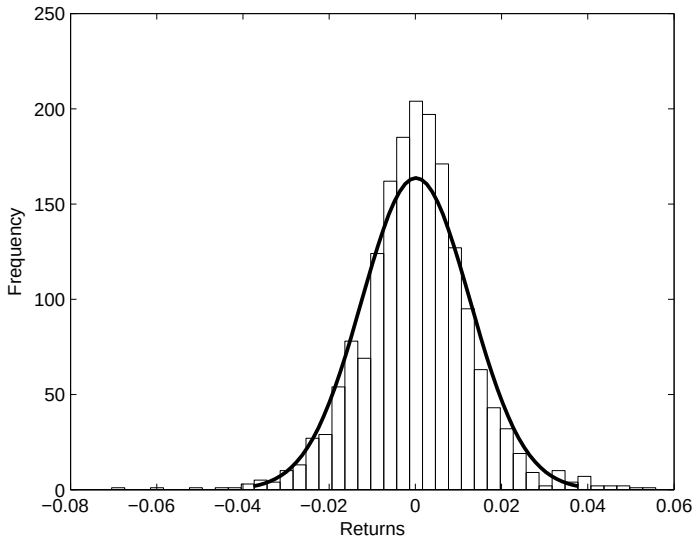

Figure 1.1: Histogram of daily SP500 log-returns

Constant volatility

In Figure 1.2 the daily log-returns for the SP500-index from 2-Jan 1998 to 31-dec 2004 are shown. We can see that the volatility seems to change over time, some periods are more volatile than others (a feature often referred to as volatility clustering). This fact is further supported by Figure 1.3 where the volatility (calculated as the standard deviation of the log-returns with a moving window of 15 days), is shown. We can see that volatility it self is volatile and changes significantly over time and that it seems to fluctuate around some long term mean-level.

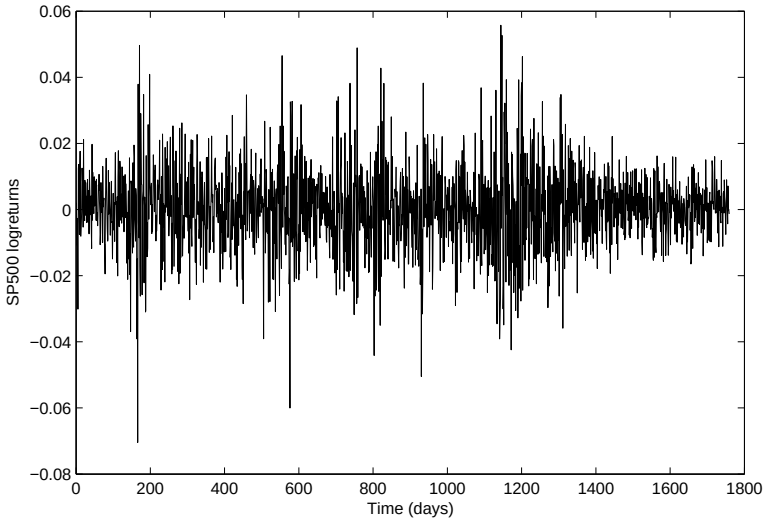

Figure 1.2: SP500 daily log-returns from 2-Jan 1998 to 31-dec 2004

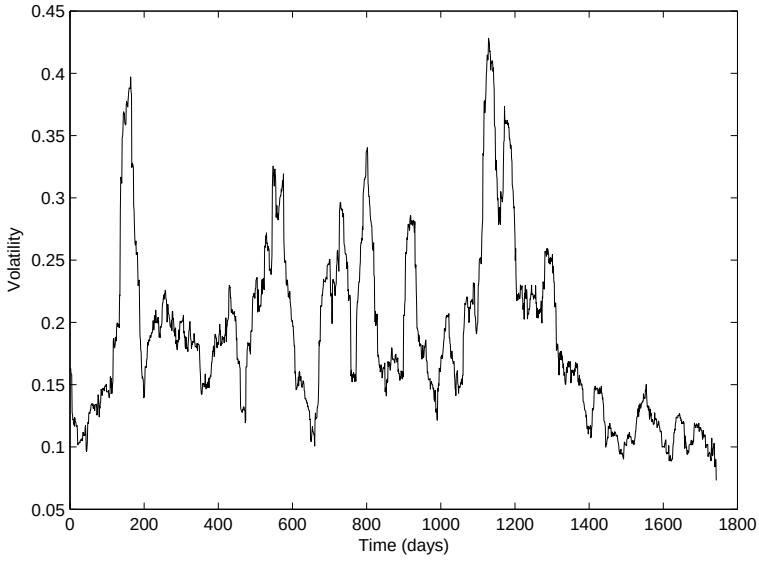

Figure 1.3: Volatility of daily SP500 returns from 2-Jan 1998 to 31-dec 2004

Volatility smile

Given a market price of an option C_M the implied volatility is defined as the volatility σ_I that inserted into the BS model will give an option price equal to the market price, i.e.

$$C_{BS}(t, S_t, K, T, \sigma_I, r) = C_M \tag{1.5}$$

Since the other model parameters are known, the implied volatility is unique and it is often used to quote option prices.
The BS model stipulates that volatility is constant, independent of other pricing parameters. This implies that all options on a specific stock should have the same implied volatility. Unfortnualy, in reality this is not the case. Instead, implied volatility empirically vary with strikes K and maturities T. The implied volatility graphed against strike for a fixed maturity is known as the volatility smile or the volatility skew. The names refers to the forms these curves often take, which may vary in different markets. Stock options for example often shows a skew effect, while in the currency world we are more likely to see a smile curve. Figure 1.4 shows the implied volatility against strike divided by current price for S&P500 options on 27-Nov 2005. The options used in the Figure have a maturity of approximately on year.
Implied volatility however also seem to vary with time to maturity, a feature commonly referred to as the term-structure of volatility. Plotting the implied volatility against both strike and time to maturity gives the so called volatility surface.
The existence of the volatility smile/surface casts a doubt over the BS model, and it is one of the reasons that several other smile-consistent model have been developed.

1.4 Alternative models

In this section we will brief the reader on some alternatives to the Black-Scholes model for the dynamics of an asset price. The models often have desirable properties that the Black-Scholes model lack, but are also more mathematically complex.

1.4.1 Lévy models

A very wide class of asset price models are models based on Lévy processes. Lévy processes are stochastic processes with independent, identically distributed increments. The class incorporate the Gaussian processes, as well as point processes, for example the Poisson process. The processes are characterized by their so called Lévy triplet (μ, σ and ν). Here, μ controls the drift of the process, σ is connected to the Gaussian component of the process. Further, ν is called the Lévy measure, controlling the frequency

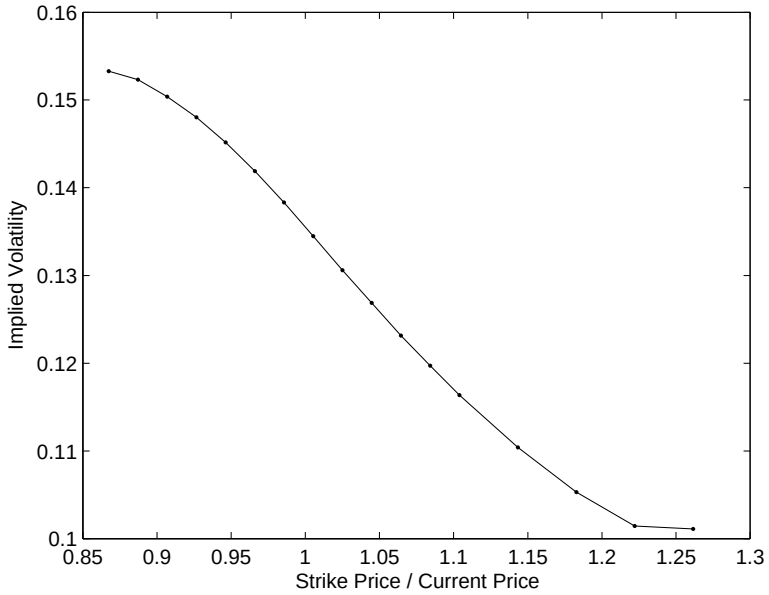

Figure 1.4: Implied volatility of SP500 options at 27-Nov 2005.

and size of the jump discontinuities of the process trajectory.

Models based on general Lévy processes can be tailored to provide a better fit to empirical data than models restricted to Gaussian driving noise. It is possible to capture traits like skewness, kurtosis and fat tails in the marginal distribution.

It is in general difficult to find replicating portfolios for derivatives in a Lévy-driven market, due to the lack of a unique risk neutral Q-measure (a concept that will be explained in Section 1.5.1).

1.4.2 Jump-Diffusion models

A less advanced improvement over the Black-Scholes framework, using discontinuities in the asset price trajectories, are the so called Jump-Diffusion models. Originating from Merton [13], these models are essentially continuous diffusions with an added point process component. The stochastic differential equation for a one-dimensional jump-diffusion process is typically of the following form

$$dS_t = \mu(S)dt + \sigma(S)dW_t + JdN. \tag{1.6}$$

Here, J is a possibly random variable controlling the size of the jumps and N is a Poisson process with constant intensity λ. In addition to the ability to incorporate instant boundary crossings, the jump component allows the model to exhibit heavy tailed marginal distributions.

To be able to construct a unique replicating portfolio, the agent must be able to trade in one distinct security per possible jump size, in addition to the stock and money market account. If J is drawn from a continuous probability distribution, infinitely many new securities must be incorporated into the model. This is not consistent with real markets.

1.4.3 Stochastic volatility models

A stochastic volatility (SV) model can be seen as a special case of the jump-diffusion model with no jump. A general SV model takes the following form:

$$\begin{aligned} dS_t =& \mu S_t dt + f(V_t) S_t dW_t^{(1)} \\ dV_t =& g(V_t)dt + h(V_t)dW_t^{(2)} \end{aligned}$$

where the two Brownian motions are correlated with correlation ρ, or, more formally:

$$[dW_t^{(1)}, dW_t^{(2)}] = \rho dt$$

where $[X, Y]$ denotes the quadratic covariation between X and Y.
Empirical evidence seem to suggest a non zero, negative, correlation ρ. Several forms for the functions $f(x)$, $g(x)$ and $h(x)$ have been suggested. Note that we here assume a constant stock-return μ. This is an assumption that of course can be relaxed. Below three stochastic volatility models are presented.

Hull & White

Hull and White [12] suggested a geometric Brownian motion for the volatility process, yielding the following model:

$$\begin{aligned} dS_t =& \mu S_t dt + \sqrt{V_t} S_t dW_t^{(1)} \\ dV_t =& \phi V_t dt + \zeta V_t dW_t^{(2)} \end{aligned}$$

A closed form solution for the European call option can be derived (see [12]) in the special case with zero correlation. This model for V_t has the advantage of always being positive.

Stein & Stein

Stein and Stein [17] modeled the process V_t by a Ornstein-Uhlenbeck (OU) process:

$$\begin{aligned} dS_t =& \mu S_t dt + |V_t| S_t dW_t^{(1)} \\ dV_t =& \alpha(\omega - V_t)dt + \beta dW_t^{(2)} \end{aligned}$$

The process V_t is mean-reverting[3] with ω beeing the long term mean, which is a feature suggested by empirical evidence. It can, however, take on negative values. Stein and Stein solved this problem by using $f(y) = |y|$. The authors provided a closed form solution for the price of a European call in the case where $\rho = 0$ (see [17]). The OU process has been used by other authors as well, Scott for example used the same dynamics of V_t, but with $f(y) = e^y$ (see [16]).

Heston

In the Heston [11] model, the driving volatility process V_t follows a CIR process. The CIR process was introduced as a model of the short rate by Cox, Ingersoll and Ross [7].

$$\begin{aligned} dS_t =& \mu S_t dt + \sqrt{V_t} S_t dW_t^{(1)} \\ dV_t =& \kappa\left(\theta - V_t\right) dt + \eta\sqrt{V_t} dW_t^{(2)} \end{aligned}$$

The Heston model is widely used, probably much due to the fact that a closed form solution exists for the European call option, regardless of the correlation ρ. This model will be examined thoroughly in the next chapter. For now, we just note that the process V_t can be shown to be strictly positive when $2\kappa\theta \geq \eta^2$, and non-negative when $0 \leq 2\kappa\theta < \eta^2$.

1.5 Pricing Methodology

In this section we look at some of the tools used when valuing derivatives.

1.5.1 Risk neutrality

In the early eighties, the concept of risk neutral measures emerged in financial theory. For some background, consider a naive approach to price a derivative, just discounting the expected payoff at a constant riskfree rate of interest. That is,

$$v_1 = \exp\{-rT\}\mathbb{E}^{\mathbf{P}}[f(S_T)]$$

[3] A mean-reverting process is pushed toward a long term mean level by its drift term, more on this concept in Section 2.3.1

where $\mathbf{P}$ is the standard probability measure observable in the real world. This approach, although intuitively attractive, is unfortunately not correct. Since the underlying asset and thus the derivative are riskier than a money market account earning the riskfree rate of interest, an investor who are risk-averse would require a premium over the riskfree rate of interest to hold the security.

But is may be shown that the price of a derivative is independent of the risk-attitude of the investor. For example, in the derivation of the pricing partial differential equations governing the price of derivatives, terms containing the drift of the underlying security disappears. The rationale for this is that as long as we may find a replicating portfolio for the derivatative, all risk is eliminated. Consider for example the Black-Scholes market, where all derivatives may be replicated by trading in the underlying stock and the money market. Not every investor have the same same risk-attitude, which means that they require a different risk premium. But if every investor may hedge a long position in a derivative by a continuously rebalanced short position in the stock, the risk premium cannot affect the replicating portfolio.

This means that we may assume that the investor is risk neutral, and only requires the stock to return the risk free rate. In order to carry out this programme, one makes a so called change of probability measure. The probability measure is a function assigning probabilities to events. The probability measure is then changed to make the stock earn the risk free rate in mean. This may be done using the Girsanov theorem, which alters the drift of a stochastic process yet leaves the volatility unchanged. In some sense, what happens is that the individual risk premium is grouped together with the driving Brownian motion, which by the Girsanov theorem now can be seen as a new Brownian motion under the changed probability measure. Since the Brownian motion is a martingale[4], and thus has no drift, the process now drifts at the risk free rate under the changed probability measure. The new measure is called the risk neutral measure, or the equivalent martingale measure, and is denoted by $\mathbf{Q}$.

Using the risk neutral measure, an approach similar to 1.7 may be used. Under $\mathbf{Q}$, the price of a derivative can be stated as

$$v_1 = \exp\{-rT\}\mathbb{E}^{\mathbf{Q}}[f(S_T)]. \tag{1.7}$$

[4]A continuous time martingale is (somewhat simplified) a stochastic process which has an expected drift of zero.

1.5.2 Model Calibration

Regardless of which model one may choose to use, one is still left with the problem of calibrating the model parameters to the market. Let $\alpha = (\alpha_1, \alpha_2, ..., \alpha_n)$ be the set of parameters for an arbitrary model. The choice of calibration method is usually a choice between two methods.

The first alternative, and perhaps the most intuitively appealing, is to calibrate the stochastic processes used in the models against observed time series data. For the Heston model, for example, this would mean obtaining stock price data and by means of some statistical inference tool fit this data to the model. This is a path taken by e.g. Ait-Sahlia and Kimmel [1], who use a maximum likelihood method for the parameter estimation. Chesney and Scott [6], use a method of moments to estimate the parameters.
This approach, however, has quite a few inherent problems. First of all, volatility itself is not an observable quantity. Hence we need to compute volatility from the data before calibrating the V_t process. A second problem we face with this approach is that the parameters obtained are valid only under the **P**-measure. This would mean that when calculating an option price from these parameters, we would have to introduce a quantity for the market price of volatility risk. Several studies suggests (see e.g. Bates [2]) that this quantity is non-zero and hence we cannot simply disregard it.
The second approach, which probably is the most used in practice and also used in this paper, is to calibrate the model so that the model's option prices p^{model} agrees with [5] the market prices p^{market}. That is, find α so that $p^{model}(\cdot\,;\alpha) = p^{market}$. By using this approach one places a great amount of confidence in effectiveness of the market, since one assumes that the market price is in fact the correct price (see Rebonato [15] for a discussion on this subject). For standard options, on liquid market, this may very well be the case. For more exotic options on the other hand, one would probably not want to put too much faith in the market prices, if such a price even exist. One could then, however, calibrate the model to standard options and then use these parameters to value more exotic options. Since we are working with market prices of options, we are in this approach working directly under the **Q**-measure and the problem of putting a number on the market price of volatility risk disappears. Mathematically this approach can be formulated as:

$$\min_{\alpha} \sum_{i=1}^{N} w_i \left(p^{model}\left(S, T_i, K_i, \alpha\right) - p_i^{market} \right)^2$$

[5] Or rather as close as possible, since in reality it is impossible to find a parameter set that retrieves the marketprices for all options.

where S is the current stock price, T is the maturity time, K the strike and N is the number of market prices used. The constants w_i, $i = 1..N$ are weights assigned to each of the options. These weights are chosen according to some scheme of ones choice. One alternative is to let the weights be a function of the bid-ask spread[6] of the market price, and hence assign a greater weight to options where the spread is small, and less weight to options with a larger spread. For this purpose we can for example chose

$$w_i = \frac{K}{p_i^{ask} - p_i^{bid}}$$

where K is the smallest bid-ask spread.

Since we have a one-to-one correspondence between option price and implied volatility, the calibration problem can also be formulated as:

$$\min_{\alpha} \sum_{i=1}^{N} w_i \left(\sigma_I^{model}(S; T_i, K_i, \alpha) - \sigma_I^{market} \right)^2 \tag{1.8}$$

where σ_I denotes the implied volatility.

1.5.3 Monte Carlo

The most intuitive approach for numerical computations of derivative prices is the Monte Carlo method. It is a fact that expectations of the form $\mathbb{E}[f(X)]$ may be approximated using the Law of Large Numbers. If the distribution of X is known, a large number of samples of X is simulated, and the expectation may be approximated using the following formula[7]

$$\mathbb{E}[f(X)] \approx \frac{1}{N} \sum_{k=1}^{N} f(x_k). \tag{1.9}$$

where $\{x_k\}_{k=1}^{N}$ are N realizations of X. If the derivative has a simple payoff function, $f(S_T)$, it is known that the price of the derivative is

$$V_0 = e^{-rT} \mathbb{E}^{\mathbf{Q}}[f(S_T)], \tag{1.10}$$

where the expectation is taken with respect to the risk neutral measure, $\mathbf{Q}$. Then, the basic idea is to generate samples of the underlying asset price at the maturity date, S_T, under the risk neutral measure. These samples can then be used to approximate the price using Equation (1.9).

For special cases, such as in the Black-Scholes model, we know the distribution of S_t and can draw samples of this value directly. In more general cases however, we are forced to revert to some kind of simulation technique. Such methods will be described in the next section.

[6] The bid-ask spread is the ask price minus the bid price.

[7] Since $\frac{x_1+x_2+\ldots+x_n}{n} \to \mathbb{E}(X)$ as $n \to \infty$

Generating asset price trajectories

The standard way to proceed to generate a sample of S_T is to simulate the whole trajectory, $(S_t)_{t\in[0,T]}$, of the asset using the underlying stochastic differential equation of the model. In this thesis, stochastic equivalents of discretization methods from ordinary differential equations is used.

Working from the initial price, S_0, a stochastic Taylor expansion of the differential equation is calculated around the starting time, t_0. Then a new value of the price process, S_{t_1}, at a nearby time point, t_1, is calculated using the Taylor expansion. Using this value as the new initial value, a new Taylor expansion is calulated around t_1 and the price at t_2 is computed using this second Taylor expansion. Continuing in this fashion, a price path is built up recursively up to the time $t_n = T$.

Below, stochastic differential equations of the following form is considered;

$$dX_t = \mu(X_t)dt + \sigma(X_t)dW_t., \tag{1.11}$$

where $\mu(\cdot)$ and $\sigma(\cdot)$ are smooth functions and W_t is a standard Brownian motion.

Euler-Maruyama discretization The simplest type of discretization method is the explicit *Euler-Maruyama* method. It is based around a first-order expansion of the differential Equation (1.11). Formally, the scheme has the following form,

$$\widetilde{X}_{t_{n+1}} = \widetilde{X}_{t_n} + \mu(\widetilde{X}_{t_n})\Delta_{t_n} + \sigma(\widetilde{X}_{t_n})\Delta W_{t_n} \tag{1.12}$$

where

$$\begin{aligned}\Delta_{t_n} &= t_{n+1} - t_n,\\ \Delta W_{t_n} &= W_{t_{n+1}} - W_{t_n} = \sqrt{\Delta_{t_n}} \times G, \quad G \sim N(0,1).\end{aligned}$$

The Euler-Maruyama scheme is intuitive and simple to implement. It works fairly well for equations where $\mu(\cdot)$ and $\sigma(\cdot)$ satisfies certain restrictive regularity conditions. For the models considered in this thesis, these conditions are unfulfilled, bringing doubt to the convergence of the scheme.

The squared error between the Euler-Maruyama discretization and the true solution, when the above mentioned conditions are fulfilled, is declining linearly with decreased stepsize Δ_t .

Higher order methods

To obtain a faster convergence to the true solution of the differential equation, a higher order Taylor approximation may be employed. The drawback is added complexity which may decrease the computation speed and make implementation harder. In this thesis we have tried a so called Milstein method, which utilizes a second order Taylor expansion. This leads to stochastic multiple integrals. The scheme looks like

$$\begin{aligned}\widetilde{X}_{t_{n+1}} = \widetilde{X}_{t_n} + \mu(\widetilde{X}_{t_n})\Delta_{t_n} + \sigma(\widetilde{X}_{t_n})\Delta W_{t_n} + \\ \frac{1}{2}\sigma(\widetilde{X}_{t_n})\sigma'(\widetilde{X}_{t_n})\left(\Delta W_{t_n}^2 - \Delta_{t_n}\right)\end{aligned} \tag{1.13}$$

The Milstein scheme converges to the true solution with order[8] 1, rather than with order 0.5 as in the Euler-Maruyama case. The error of the scheme thus tends to zero linearly with decreased stepsize.

1.5.4 Partial differential equation pricing methods

In general, while Monte Carlo may be easy to implement and understand, it lacks the speed sometimes needed to price derivatives in practice. Since the method scales well to high dimension, it is most commonly used for multifactor models. For models with one or two factors, such as the models described in this thesis, an alternative method is to set up a partial differential equation (PDE) governing the price of the derivative. We then use standard numerical methods, such as finite differences or finite elements, to solve the PDE subject to various boundary and initial conditions. This can sometimes be more computationally efficient. In this thesis we have tried an explicit finite difference approach for the Heston stochastic volatility model. Since this is a two-factor model, we have to work with a three-dimensional PDE, with one time dimension and two spatial dimension corresponding to the volatility and the asset price respectively.

Finite Difference Method

Heston, [11], derives a partial differential equation for $f(s,t)$ when S_t satisfy Equation 2.1 and $f(s,t)$ is the price of a derivative at time t, given that $S_t = s$. The derivative contract is defined in terms of the boundary and

[8] A method is said to have order of convergence equal to α if there exists a constant C such that $\mathbb{E}(|\widetilde{X}_{t_n} - X(t_n)|) \leq C\Delta_t^{\alpha}$. I.e the higher the order of convergence, the more the error decreases when the stepsize is decreased.

initial conditions of the partial differential equation. The PDE is given by

$$\frac{\partial f}{\partial t} = \frac{1}{2}v\left(\frac{\partial^2 f}{\partial S^2} + \eta^2\frac{\partial^2 f}{\partial v^2} + 2\rho\eta\frac{\partial^2 f}{\partial S \partial v}\right) - \left(\frac{1}{2}v - r\right)\frac{\partial f}{\partial S} + \kappa(\theta - v)\frac{\partial f}{\partial v} - rf \tag{1.14}$$

To solve an equation such as 1.14, we apply a finite difference scheme. First we set up a space-time grid on which we will discretize the equation. We let time run from 0 to T, and partition the time line into M intervals of equal length. In the asset and volatility directions, we choose bounds for the grid of the form S_{min}, S_{max} and v_{min}, v_{max} and then partition these intervals into N intervals each of equal length in each direction. Counting the lower boundaries, we then have a three-dimensional grid with $(M+1)\times(N+1)\times(N+1)$ points; $\{t_0, t_1, \ldots, t_M\}\times\{S_{min} = S_0, S_1, \ldots, S_N = S_{max}\}\times\{v_{min} = v_0, v_1, \ldots, v_N = v_{max}\}$. Let $\Delta_S = S_n - S_{n-1}$, $\Delta_v = v_k - v_{k-1}$ and $\Delta_t = t_l - t_{l-1}$.

We then approximate the derivatives in the spatial direction with so called central differences. For notational convenience, we let $f(t_n, S_k, v_l) = f_{n,k,l}$. Now let

$$\frac{\partial f_{n,k,l}}{\partial S} \approx \frac{f_{n,k+1,l} - f_{n,k-1,l}}{2\Delta_S} \tag{1.15}$$

$$\frac{\partial f_{n,k,l}}{\partial v} \approx \frac{f_{n,k,l+1} - f_{n,k,l-1}}{2\Delta_v}. \tag{1.16}$$

For the second order derivatives, we let

$$\frac{\partial^2 f_{n,k,l}}{\partial S^2} \approx \frac{f_{n,k+1,l} - 2f_{n,k,l} + f_{n,k-1,l}}{\Delta_S^2} \tag{1.17}$$

$$\frac{\partial^2 f_{n,k,l}}{\partial v^2} \approx \frac{f_{n,k,l+1} - 2f_{n,k,l} + f_{n,k,l-1}}{\Delta_v^2} \tag{1.18}$$

$$\frac{\partial^2 f_{n,k,l}}{\partial S \partial v} \approx \frac{f_{n,k+1,l+1} + f_{n,k-1,l-1} - f_{n,k+1,l-1} - f_{n,k-1,l+1}}{4\Delta_S\Delta_v} \tag{1.19}$$

In the time direction we use a so called explicit time step. Since we are letting time flow backwards in the valuation procedure, the difference approximation becomes

$$\frac{\partial f_{n,k,l}}{\partial t} \approx \frac{f_{n,k,l} - f_{n+1,k,l}}{\Delta_t} \tag{1.20}$$

Inserting the approximations (1.15) - (1.19) in the PDE (1.14) and simpli-

fying, we end up with the following relation,

$$f_{n,l,k} = \begin{pmatrix} \xi_{k-1,l-1} & \xi_{k,l-1} & \xi_{k+1,l-1} \end{pmatrix} \cdot \begin{pmatrix} f_{n+1,k-1,l-1} \\ f_{n+1,k,l-1} \\ f_{n+1,k+1,l-1} \end{pmatrix} + \begin{pmatrix} \xi_{k-1,l} & \xi_{k,l} & \xi_{k+1,l} \end{pmatrix} \cdot \begin{pmatrix} f_{n+1,k-1,l} \\ f_{n+1,k,l} \\ f_{n+1,k+1,l} \end{pmatrix} + \begin{pmatrix} \xi_{k-1,l+1} & \xi_{k,l+1} & \xi_{k+1,l+1} \end{pmatrix} \cdot \begin{pmatrix} f_{n+1,k-1,l+1} \\ f_{n+1,k,l+1} \\ f_{n+1,k+1,l+1} \end{pmatrix} \tag{1.21}$$

where the ξ-components are time-independent coefficients, completely defining the function f on the t_n-space grid in terms of the function values on the t_{n+1}-space grid. Thus we may recursively work backwards from the date of maturity to approximate the PDE on the whole three-dimensional grid. The exact formulation of the space grid coefficients is

$$\begin{aligned}
\xi_{k-1,l-1} &= p(\rho\eta\frac{l}{4h}) \\
\xi_{k,l-1} &= p(\frac{l}{2h}\eta^2 + \frac{\kappa}{2}l - \frac{\kappa\theta}{2h}) \\
\xi_{k+1,l-1} &= -p(-\rho\eta\frac{l}{4h}) \\
\xi_{k-1,l} &= p(\frac{1}{2h}l) \\
\xi_{k,l} &= -1 - \frac{pl}{h}(1+\eta^2) + \frac{p}{2}lh \\
\xi_{k+1,l} &= \frac{p}{2h} \\
\xi_{k-1,l+1} &= -\rho\eta p\frac{l}{4h} \\
\xi_{k,l+1} &= p(\frac{l}{2h}\eta^2 - \frac{\kappa}{2}l + \frac{\kappa\theta}{2h}) \\
\xi_{k+1,l+1} &= p\rho\eta\frac{l}{4h},
\end{aligned}$$

where $p = \Delta_S = \Delta_v$ and $h = \Delta_t$.

1.5.5 Lattice methods

Rather closely connected with the PDE method, the lattice approach is based on the idea to build up a tree of possible asset price paths and then calculate the price of the derivative recursively from the date of maturity and going backwards to the starting date. Most often, for one-factor models, the trees are binomial or trinomial.

Quadrinomial trees

To account for two-factor models, it is needed to build up three-dimensional trees. For the stochastic volatility case, Guan [10] describes a method to price options with early exercise possibilities using such quadrinomial lattices.

Here follows a short introduction to the methodology. As for the finite difference method, we start by partitioning the domain in a three-dimensional grid; $\{t_0, t_1, \ldots, t_M\} \times \{S_{min} = S_0, S_1, \ldots, S_N = S_{max}\} \times \{v_{min} = v_0, v_1, \ldots, v_N = v_{max}\}$. For each point on the grid, jump sizes and jump probabilities are calculated. In Guan [10], formulas for this is provided for the Heston case. We name the jump sizes U_S, D_S, U_v, D_v for up and downwards asset price jump and up and downwards volatility jumps respectively. The joint jump probabilites is denoted $\rho_{1,1}, \rho_{1,2}, \rho_{2,1}, \rho_{2,2}$, representing *up-up*,*up-down*,*down-up*,*down-down*.

Now, at time t_{n-1}, the value of $f_{n-1,k,l}$ may be calculated as

$$\begin{aligned} f_{n-1,k,l} = \big(&\rho_{1,1} f(t_n, S_k + U_S, v_l + U_v) + \\ &\rho_{1,2} f(t_n, S_k + U_S, v_l + D_v) + \\ &\rho_{2,1} f(t_n, S_k + D_S, v_l + U_v) + \\ &\rho_{2,2} f(t_n, S_k + D_S, v_l + D_v)\big)/(1 + r) \end{aligned} \tag{1.22}$$

where r is the short rate of interest. The problem is that $f(t_n, S_k + U_S, v_l + D_v)$ seldom lies on the t_n-space grid. In order to cope with this difficulty, the option values which lies between grid points are interpolated using some algorithm. We have tried both a simple linear interpolant as well as the Matlab *interp2*-routine with cubic spline interpolation. For function evaluations outside the grid boundaries, extrapolation have been used. For the call option, we should have that $\frac{\partial f}{\partial S} \approx 0$ when S is large. This makes extrapolation on the outer S-boundary easy.

1.5.6 Pricing Path Dependent Options using Monte Carlo

The pricing of path dependent derivatives is most easily done with Monte Carlo methods. The lattice and PDE methods is limited by the fact that the price in these settings is recursively computed from the date of maturity and backwards. This makes it hard to capture the effects of for example boundary crossings, which propagates forward in time. This is comparable to the case with the usual forward-running heat equation with a maturity condition, which is an illposed problem.

Nonadjusted running extremes

The first approach we use in this paper is not adjusted to deal with the errors following from the discrete monitoring of the price-path. We generate the trajectories in the same manner as for the European call option case, setting up a partition of the time interval up to the date of maturity, $0 = t_0 < t_1 < \ldots < t_{n-1} < t_n = T$, and approximate the driving differential equation on these partition points using the modified[9] Euler method for the volatility path and the usual Euler method for the asset price path.

In addition, for each path, we compare the value of the solution at each point with the condition introduced by the path-dependency. For a up-and-out (call) barrier option, for example, we compare the value with the upper boundary. If the path stays below this boundary, ub, for each point, the derivative has a payoff equal to a European call on the date of maturity. Should the path hit or cross over the boundaries, the algorithm returns zero. Then the mean of the payoffs is taken and this value is then discounted to the present date. Formally, the price of a up-and-out call option is approximated by

$$V(t_0) \approx e^{-r(T-t_0)} \frac{1}{N} \sum_{k=1}^{N} \mathbf{1}_{\{(S_k(t_l))_{l=0}^{n} < ub\}} \times (S_k(T) - K)^+ \tag{1.23}$$

where N is the number of simulated trajectories.

Adjusted running extremes

The second approach tries to remedy the problems inherent with monitoring a continuous path through discrete approximation. Comparing the path at the simulation time points with the boundary implies that one interpolates the process between the points using piecewise linear interpolants. Because of the non-zero quadratic variation of the true solution, this will underestimate the running maximum and overestimate the running minimum of the solution.

In Glasserman [9] the problem is tackled by assuming that the process between two consecutive points may be approximated by a Brownian motion. Conditioning on the process value at t_{n-1} and t_n we connect the points with a standard Brownian bridge. The distribution of the maximum over a Brownian bridge is known, and we can simulate is using the following formula (see [9]).

$$\widetilde{M}_n = \frac{S_n + S_{n-1} + \sqrt{(S_n - S_{n-1})^2 - 2\sigma^2 V_{n-1} \Delta_t \log U_n}}{2}, \tag{1.24}$$

[9]This modification is to ensure the variance process stays positive, and it will be described in Section 2.2.

where U_n is a uniformly distributed variable on $[0, 1]$. The minimum over the Brownian bridge may be simulated using a similar formula.

Chapter 2

The Heston model

2.1 Introduction

In this chapter we will study the Heston stochastic volatility model. We will look at the features of the model, and give a closed form solution for the price of a European call option. Using this formula we show that the Heston model can reproduce a smile-like implied volatility curve, similar to the ones encountered in market.

We remind the reader of the processes underlying the Heston model,

$$\begin{aligned} dS_t =& \mu S_t dt + \sqrt{V_t} S_t dW_t^{(1)} \\ dV_t =& \kappa\left(\theta - V_t\right) dt + \eta\sqrt{V_t} dW_t^{(2)} \end{aligned} \tag{2.1}$$

where

$$[dW_t^{(1)}, dW_t^{(2)}] = \rho dt.$$

A description of the coefficients and features of the model will be given in Section 2.3 below.

2.2 Simulation

In Figure 2.1 a sample trajectory of the variance process V_t is shown. The simulation is done using an Euler scheme, with the following parameters: $V_0 = 0.0082$, $\theta = 0.0168$, $\kappa = 6.21$, $\eta = 0.625$, $\rho = -0.6674$ and with the discretization time step $\Delta_t = 2^{-15}$. In order to keep the process V_t from becoming negative, a minor modification to the Euler method was implemented. We simply check if $\widetilde{X}_{t_{n+1}} < 0$ and then ignore the value and perform a new simulation step.

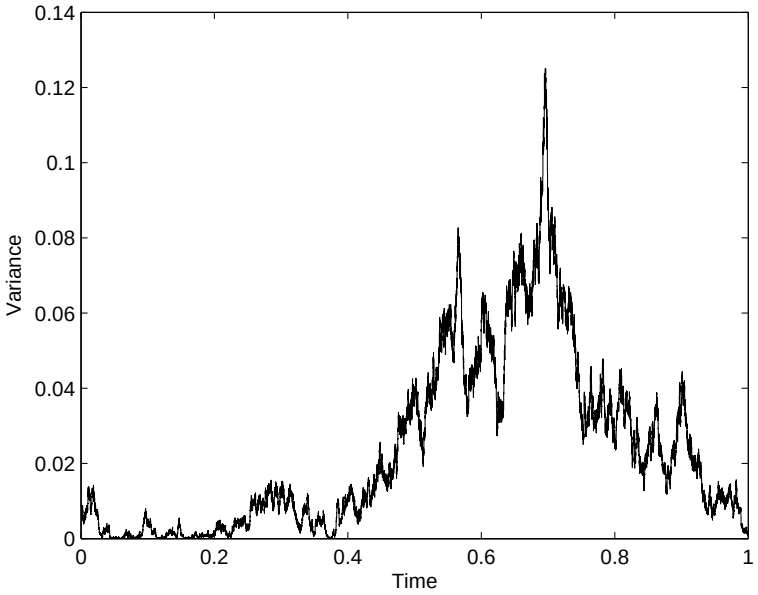

Figure 2.1: Simulation of V_t

In Figure 2.2 a trajectory of the price process S_t corresponding to the V_t sampling from Figure 2.1 is shown. We note that S_t is more volatile when V_t takes a large value, and vice versa.

2.3 Features

2.3.1 Mean reversion

Looking at the drift term (the dt-term) in Equation (2.1) we see that the process is mean-reverting when $\kappa > 0$, with θ being the mean-level. That is, when the process value V_t is less than θ the drift term will push the process value up, and the reverse argument applies when the process value is greater then the mean-level. Mean reversion of the volatility process was justified by looking at empirical findings in Section 1.3.2, but can also be motivated by a simple argument. Suppose the process was not mean-reverting, and that we today have a volatility level of for example 20%. Without mean reversion, there would be a low probability that the process would be within resonable levels, for example 1% and 100% after a period of time. And since it is fairly reasonable to assume that this will be the case, mean reversion makes sence.

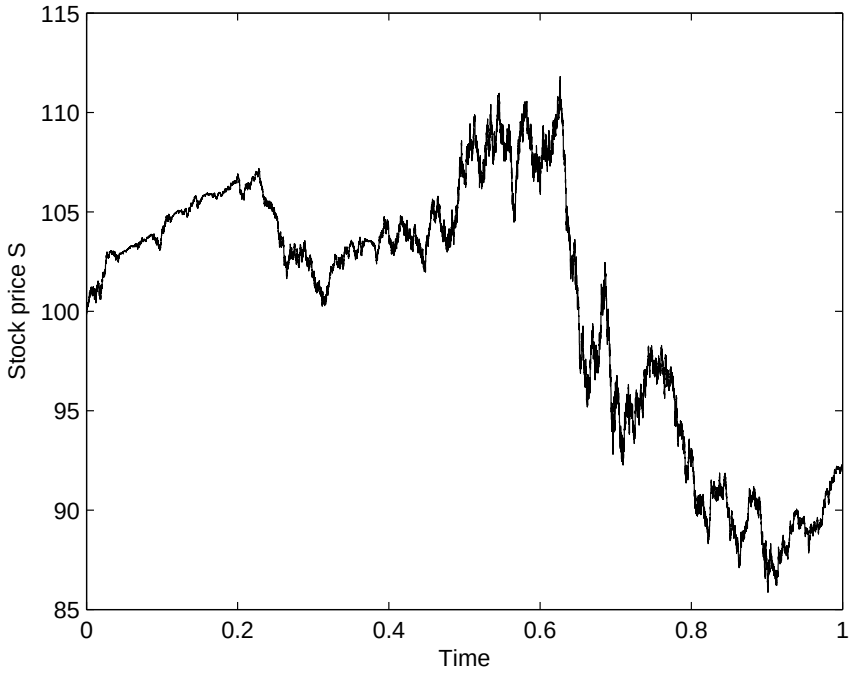

Figure 2.2: Simulation of S_t

2.3.2 Correlation

Empirical studies has suggested that the price process and the volatility process of stocks should be negatively correlated, i.e. market volatility increases when prices goes down, and vice versa. The value and especially the sign of the correlation affects the distribution of the returns. A negative correlation yields a left-tail-skewness, i.e. the left tails is fatter than the right tail. This is empirically supported, with large price declines being more frequent than large price gains. In Figure 2.3 a histogram of returns simulated form the Heston model with correlation $\rho = -0.6674$ using an Euler-scheme is shown. We see that the tail are fatter than in an normal distribution, and that the distribution is more peaked around the center. From Section 1.3.2 we know that these are features we see in market data.

2.3.3 Model Parameter

In summary, the Heston volatility process has the following parameters:

- κ - Mean reversion speed. For the process to be mean reverting, we need $\kappa > 0$.
- θ - The long term mean level of the variance V_t.

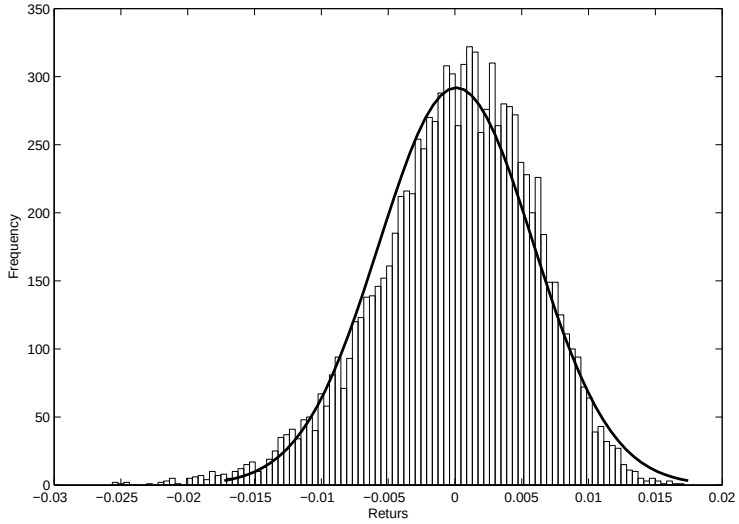

Figure 2.3: Histogram of returns simulated from the Heston model.

- η - The volatility of V_t, i.e. the volatility of the volatility.
- ρ - The correlation between the Brownian motion driving the stock-price process S_t and the Brownian motion driving the variance process V_t.
- V_0 - The starting value of the variance process.

As mentioned earlier, the condition $2\kappa\theta \geq \eta^2$ ensures that the process V_t is strictly positive, while $0 \leq 2\kappa\theta < \eta^2$ keeps it non-negative.

2.4 Derivatives pricing

2.4.1 European call options

In the Heston model, we can derive a closed form solution to the price of a European call option. The complete derivation is quite technical, and the interested read can find it in Heston [11].
Let $c(x, v, \tau)$ be the price of a European call option, maturing at time T, at the current time t and let $\tau = T - t$. Further let r denote the risk free rate, S_0 be the current price of the stock, F the forward price of the stock to expiry (i.e. $F = S_0 e^{r\tau}$), K the strike, $x = \ln(\frac{F}{K})$ and v the current volatility level (i.e. V_0 if we let $t = 0$). Then the price of the option can be expressed as,

$$c(x, v, \tau) = Ke^{-r\tau} \left(e^x P_1(x, v, \tau) - P_0(x, v, \tau) \right), \; j = 1, 2 \tag{2.2}$$

where

$$\begin{aligned}
P_j(x, v, \tau) &= \frac{1}{2} + \frac{1}{\pi} \int_0^\infty \Re \left(\frac{e^{C_j(k,\tau)\theta + D_j(k,\tau)v + ikx}}{ik} \right) dk \\
D_j(k, \tau) &= r_- \frac{1 - e^{-d\tau}}{1 - ge^{-d\tau}} \\
C_j(k, \tau) &= \kappa \left(r_- \tau - \frac{2}{\eta^2} \ln \left(\frac{1 - ge^{-d\tau}}{1 - g} \right) \right) \\
g &= \frac{r_-}{r_+} \\
r_\pm &= \frac{\beta \pm d}{\eta^2} \\
d &= \sqrt{\beta^2 - 4\alpha\gamma} \\
\alpha &= -\frac{k^2}{2} - \frac{ik}{2} + ijk \\
\beta &= \kappa - \rho\eta j - \rho\eta ik \\
\gamma &= \frac{\eta^2}{2}
\end{aligned}$$

Above $\Re(z)$ denotes the real part of the complex number z, and $i^2 = -1$. The integral above does not have a primitive function, and therefore has to be solved numerically.

The smile

One of the desirable features of the Heston model is that we can reproduce the implied volatility smiles/skews encountered in the market (see Section 1.3.2). Figure 2.4 show the implied volatility against strike for three different correlations ρ. The options have a maturity of one year, and the parameters are, $S_0 = 100$, $r = 3\%$, $V_0 = 0.0082$, $\theta = 0.0168$, $\kappa = 6.21$, $\eta = 0.625$.
We see that the correlation affects the shape and especially the slope of the implied volatility curve. A negative correlation leads to a downward sloping curve. Intuitively this makes sense, since as mentioned earlier a negative correlation increases the fatness of the downward tail in relation to the upward tail in the distribution of the stock returns. It is then reasonable to think that this leads to a higher value of puts that are far out of money (i.e. $K < S_0$). Thus because of the put call parity, the call options will also increase in implied volatility.

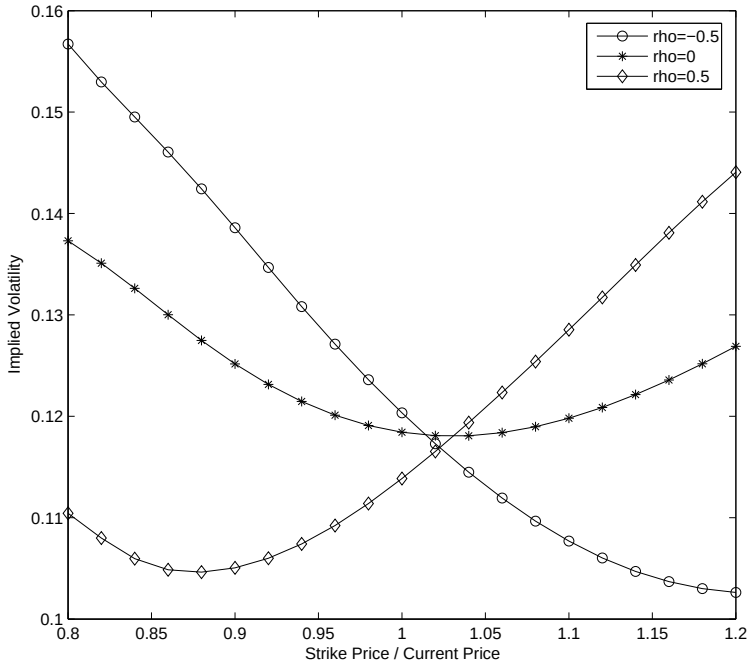

Figure 2.4: Implied volatility curves produced by the Heston model.

Chapter 3

Results

3.1 Introduction

In this chapter we fit the Heston model to market data. We then use the parameters obtained from the calibration to price some exotic derivatives, mainly using Monte Carlo simulation. This include sensitivity analysis. We also assess the effectivness of Monte Carlo pricing in the Heston model in the case of a European Call option, where we have a closed form solution to compare with.

All implementations presented in this chapter have been done in Matlab and C++, where the latter was used mainly in computationally demanding calculations, such as Monte Carlo simulations.

3.2 Model calibration

When calibrating the Heston model against market data, we follow the second route described in Section 1.5.2. That is, we choose the parameters that produces the best fit of the theoretical prices compared to the corresponding market price. This means that we are faced with the following optimization problem,

$$\min_{\alpha} \sum_{i=1}^{N} \left(\sigma_I^{model}\left(x, \tau_i, K_i; \alpha\right) - \sigma_I^{market} \right)^2 \tag{3.1}$$

where

$$\alpha = (V_0, \theta, \kappa, \eta, \rho).$$

and σ_I denotes the implied volatility, defined as in Equation (1.5). We choose to calibrate our model against the SP500 index, mainly due to the fact that there exist a very liquid market in options written on this index.

We use the closing prices from 29-Sept 2005, calculated as the mean of the bid and ask price. Options with a too wide bid-ask spread were disregarded. These were mainly options that were either far in the money, or far out of the money. This approach is equivalent to setting w_i in Equation (1.8) to either zero or one depending on the size of the bid-ask spread.

We chose to calibrate only to one specific maturity of approximately one year, i.e. $\tau_i = \tau_j \approx 1$ for $i, j = 1..N$.

The minimization problem (3.1) is by no means an easy problem, since the objective function has many local minimums[1]. Hence the solution is very sensitive to the choice of the initial starting point α_0 in the optimization. We used different values of α_0, obtained from earlier papers on the subject (e.g. Duffie et al. [8] and Byström[2] [5]). We also varied one of the starting parameters while holding all others fixed. Manually evaluating the optimal solutions produced by all optimizations yielded the following parameter set $\widehat{\alpha} = (v_0, \theta, \kappa, \eta, \rho)$ as the best fit,

$$\begin{aligned} v_0 &= 0.0082 \\ \theta &= 0.0168 \\ \kappa &= 6.21 \\ \eta &= 0.625 \\ \rho &= -0.6674 \end{aligned}$$

Note that the condition $2\kappa\theta \geq \eta^2$ which ensures that V_t is strictly positive is not fulfilled. However we do have that $0 \leq 2\kappa\theta < \eta^2$, the condition required for V_t to be non-negative. These parameters coincide well with the parameters obtained in Duffie et al. [8]. In order to perform yet another test of the validity of the parameters, we re-calibrated the model at a later time, 25-Nov 2005. The parameters obtained from this calibration were exactly the same, apart from θ, which differed only in the last decimal. This observation supports the time stationarity of the variance parameters.

In Figure 3.1, SP500 call option implied volatility from the close of 25-Nov 2005 is plotted together with implied volatilities suggested by the Heston model (i.e. Equation (2.2)) with the parameter set $\widehat{\alpha}$). We see that the market implied volatility is very close to the model suggested implied volatility for options that are at the money. The spread then widens as we move more

[1] See for example Mikhailov and Nögel [14] for a discussion of this. Mikhailov and Nögel also suggests a stochastic optimization algorithm - the so called simulated annealing algorithm - as a way of solving this issue.

[2] Byströms calibrated the Heston model to Swedish OMX options. Still, we tested the parameters as initial values, since it is not unreasonable to believe that the volatility of the OMX index is quite similar to that of the SP500.

into the money, as well as out of the money, with the latter giving a better fit.

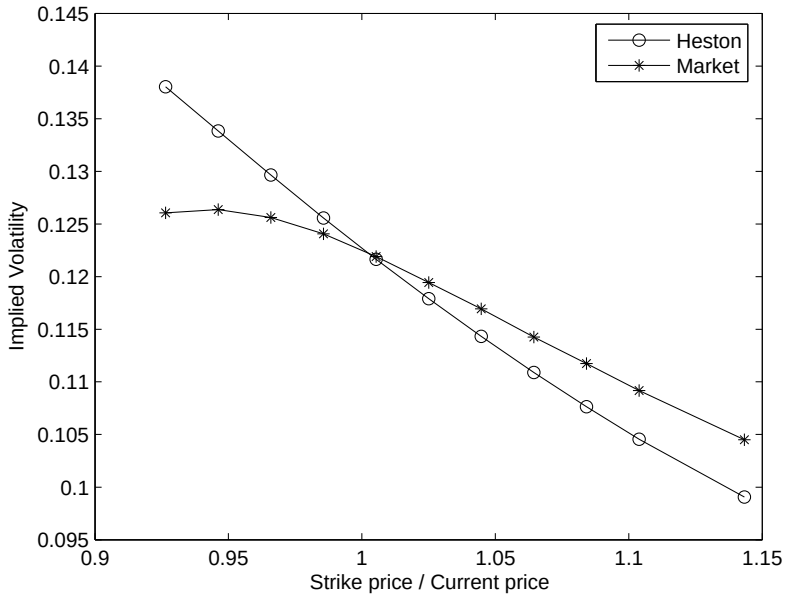

Figure 3.1: SP500 implied volatility and model implied volatility on 25-Nov 2005

3.3 European call options

3.3.1 Pricing

In absence of dividends, Equation (2.2) provides a closed form solution for the price of a European call option in the Heston model. In order to assess the effectiveness of Monte Carlo (MC) pricing under stochastic volatility we compared the price produced by the closed form against the price from a Monte Carlo simulation. The simulations of V_t and S_t were done using an Euler-Maruyama scheme, with steplength $\Delta_t = \frac{1}{2^{15}}$. The parameters used for the variance process V_t were $\widehat{\alpha} = (v_0, \theta, \kappa, \eta, \rho) = (0.0082, 0.0168, 6.21, 0.625, -0.6674)$ and the current stock price $S_0 = 100$, strike price $K = 100$, interest rate $r = 4\%$ and time to maturity $T = 1$ year. Feeding these numbers into Equation (2.2) yields the option price $C_{CF} = 6.9990$.
Table 3.1 shows the prices produced by the Monto Carlo pricing function for a different number of sample trajectories N together with the deviation from the price C_{CF} in percent.

N	*MC Price*	*Difference (%)*
1000	6.7290	−3.859
10000	6.9073	−1.311
20000	6.8821	−1.671
40000	6.8896	−1.564
80000	6.9303	−0.982
120000	6.8900	−1.558

Table 3.1: Call option prices calculated using Monte Carlo. Here $C_{CF} = 6.9990$

We see that the differences between the MC method and the closed form solution are quite large. We also note that all MC prices are smaller than the closed form price, and that the difference does not seem to decrease when the number of simulations are increased.
The above results raises suspicion that the MC method consistently puts a downward bias on the option price. To check if this seems to be the case, a second test was preformed. In this test, 71 MC prices were calculated, all using a steplenght of $\Delta_t = \frac{1}{2^{14}}$ and the number of simulations $N = 10000$. Of the 71 prices produced, 70 were below the closed form price C_{CF} and only one were greater. The mean percent deviation from the closed form price were -2.3%. Hence it seems fairly likely that the Monte Carlo approximation puts a downward bias on the option price. Broadie and Kaya [4] obtain a similar bias. They explain this mainly by a discretizatin error occuring when the simulated variance process V_t hits zero or a negative number. Recall that, as described in Section 2.2, we have to make a modification to the Euler-Maruyama scheme to keep the process positive. The authors also state that this discretization error is especially noticable when $2\kappa\theta \leq \eta^2$, which is the case for our parameters $\widehat{\alpha}$.

3.3.2 Sensitivity analysis

Correlation

In Figures 3.2 and 3.3 the price of a European call option, calculated using Equation (2.2), is plotted against correlation ρ for two different strikes, $K = 85$ and $K = 115$. The current stock price is $S_0 = 100$. Hence Figure 3.2 shows an option that is in the money, while Figure 3.3 shows an option that is out of the money. The parameters used for the variance process are $\widehat{\alpha} = (v_0, \theta, \kappa, \eta) = (0.0082, 0.0168, 6.21, 0.625)$. The time to maturity is one year, and the risk free interest rate is 4%.

We see that for the option that is in the money, the price is **decreasing** in ρ, while for the option that is out of the money, the price is **increasing**

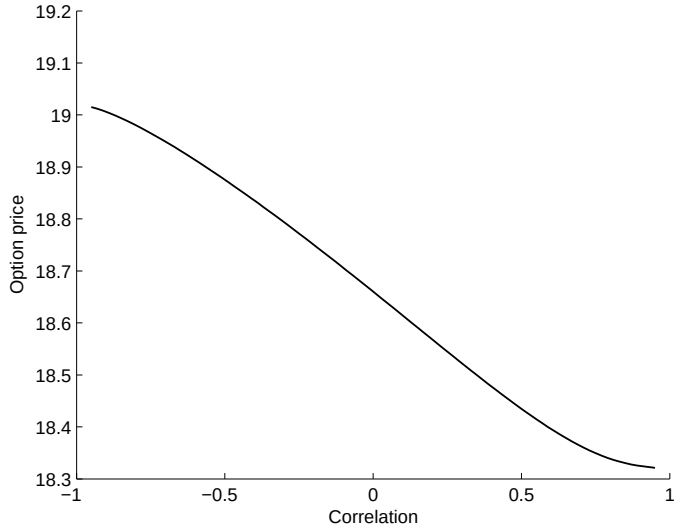

Figure 3.2: Call option price against correlation for $K = 85$ and $S_0 = 100$.

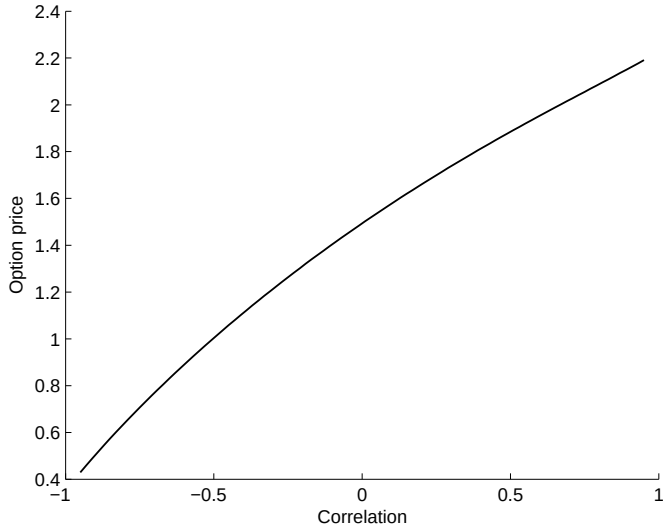

Figure 3.3: Call option price against correlation for $K = 115$ and $S_0 = 100$.

in ρ. It is worth noticing that the price of the out of the money option (Figure 3.3) varies a great deal with correlation. The price with a large positive correlation is three times as big as the price with a strong negative correlation. This feature is not shared with the in the money option, where the price varies only little with respect to correlation.

Greeks

From Equation (2.2) we can derive an expression for the delta of a European call option in the Heston model. First we differentiate (2.2) with respect to x to obtain

$$\frac{\partial c(x,v,\tau)}{\partial x} = Ke^{-r\tau}\left(e^x P_1(x,v,\tau) + e^x P_1'(x,v,\tau) - P_0'(x,v,\tau)\right)$$

where $P_j(x,v,\tau)$ is defined as in Equation (2.2) and

$$P_j'(x,v,\tau) \equiv \frac{\partial P_j(x,v,\tau)}{\partial x} = \frac{1}{\pi}\int_0^\infty \Re\left(e^{C_j(k,\tau)\theta + D_j(k,\tau)v + ikx}\right) dk$$

Now we recall that,

$$x = \ln\left(\frac{Se^{r\tau}}{K}\right)$$

Hence, using the chain rule, we arrive at the following expression for the delta of a European call option in the Heston model,

$$\Delta_H = \frac{\partial c(x,v,\tau)}{\partial S} = \frac{\partial c(x,v,\tau)}{\partial x} \times \frac{\partial x}{\partial S} = \tag{3.2}$$
$$\frac{1}{S} \times Ke^{-r\tau}\left(e^x P_1(x,v,\tau) + e^x P_1'(x,v,\tau) - P_0'(x,v,\tau)\right)$$

In the same manner we can derive the following expression for the gamma of a European call option in the Heston model,

$$\Gamma_H = \frac{\partial^2 c(x,v,\tau)}{\partial S^2} = \tag{3.3}$$
$$\frac{1}{S^2} \times Ke^{-r\tau}\left(e^x P_1'(x,v,\tau) + e^x P_1''(x,v,\tau) + e^x P_0'(x,v,\tau) - P_0''(x,v,\tau)\right)$$

where

$$P_j''(x,v,\tau) \equiv \frac{\partial^2 P_j(x,v,\tau)}{\partial x^2} = \frac{1}{\pi}\int_0^\infty \Re\left(ike^{C_j(k,\tau)\theta + D_j(k,\tau)v + ikx}\right) dk$$

In Figures 3.4 and 3.5, Δ_H is plotted against the moneyness ratio S/K. In Figure 3.4 the correlation is negative, $\rho = -0.6674$, while in Figure 3.5 the correlation is positive, $\rho = 0.6674$. Both graphs share the properties $K = 100$, $r = 3\%$, $T = 0.5$ years, $V_0 = \theta = 0.0168$, $\kappa = 6.21$ and $\eta = 0.625$. In the same figures the Black-Scholes delta Δ_{BS} is shown as well. The volatility used to calculate Δ_{BS} is the same as V_0 and θ, i.e. $\sigma = \sqrt{0.0168} = 0.1296$.

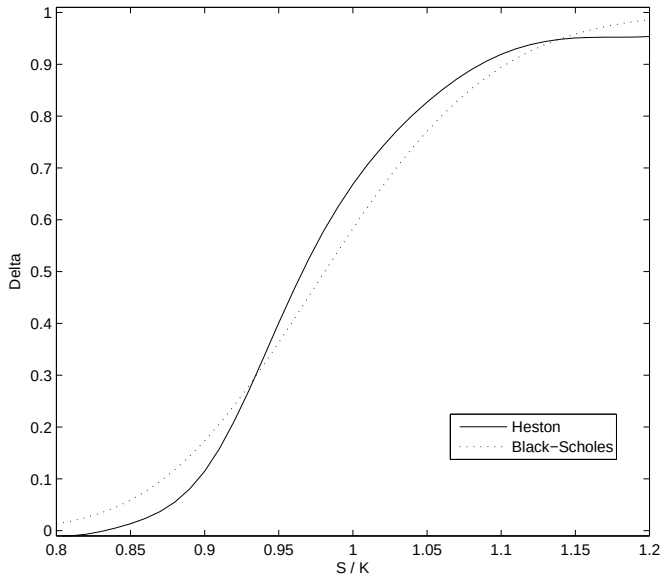

Figure 3.4: Δ_H and Δ_{BS} against S/K for $T = 0.5$ with negative correlation $\rho = -0.6674$.

We notice the difference in curvature depending on the correlation ρ. This becomes more apparent in Figures 3.6 and 3.7 which shows the gamma Γ_H and Γ_{BS} for the same set of parameters. We see that changing from negative to positive correlation seems to mirror the gamma around some point $S/K \approx 1$. For a positive correlation the maximum of the gamma lies where $S/K > 1$, i.e. in the money. For negative correlation however, as well as for the Black-Scholes, the maximum is slightly out of the money, i.e. $S/K < 1$.

3.4 American options

Unfortunately, although great efforts were made, we did not succeed in implementing a working pricer for the American options. Both the finite dif-

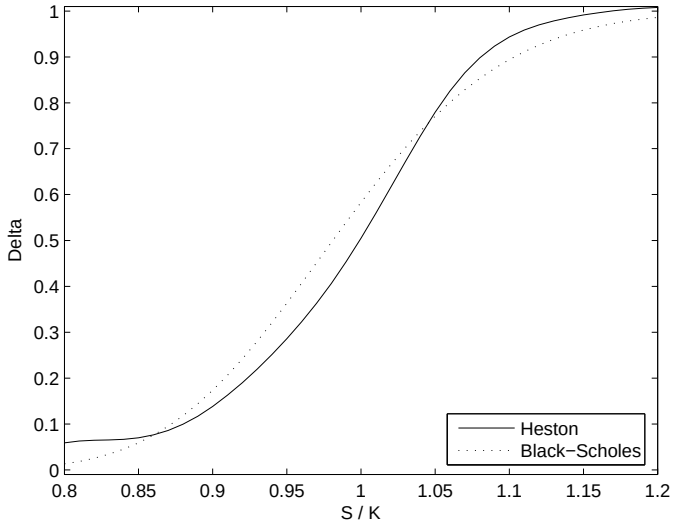

Figure 3.5: Δ_H and Δ_{BS} against S/K for $T = 0.5$ with positive correlation $\rho = 0.6674$.

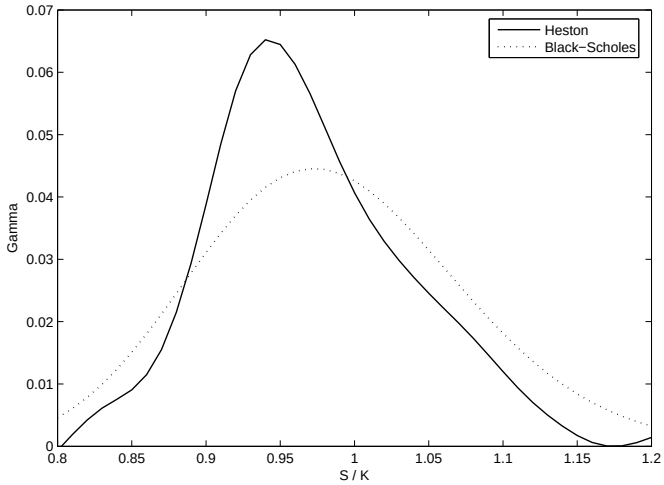

Figure 3.6: Γ_H and Γ_{BS} against S/K for $T = 0.5$ with negative correlation $\rho = -0.6674$.

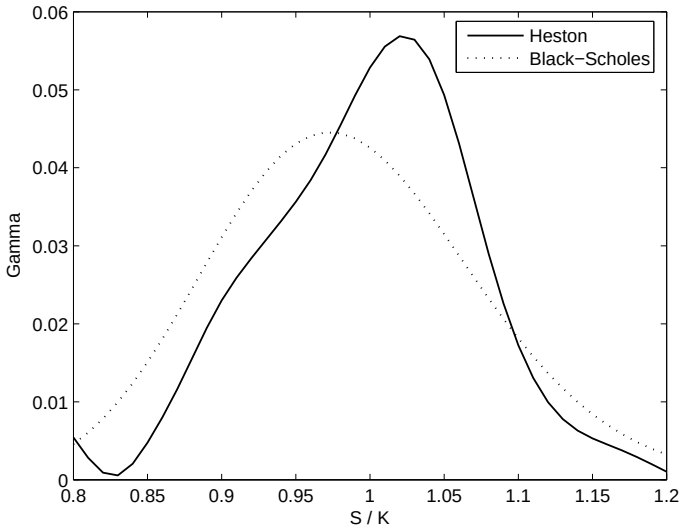

Figure 3.7: Γ_H and Γ_{BS} against S/K for $T = 0.5$ with positive correlation $\rho = 0.6674$.

ference and the lattice methods were tested. Below, we give some details of what went wrong and which problems that occurs.

3.4.1 Finite Differences

The finite difference solver we developed displays extreme instability problems. Even using such a small time step as $\Delta_t = C\Delta_S^4$ could not resolve the instabilities for space grids larger than about 8×8. A working strategy may be to use implicit time steps, either fully implicit or Crank-Nicholson differencing. Because of the added complexity, we have not tried this approach.

3.4.2 Quadrinomial Lattices

The lattice method did not seem to work properly for us. Using a naive linear interpolation step, the general shape of the $S \times v$-surface looks fine, but the slope in the S-direction increased more and more as the algorithm moved backwards through time. This is not consistent with theory which suggests that the slope should be equal to one for large S. The behavior was present even when the extrapolation step used a slope of 1 to compute values outside the S-range.

Using the cubic spline-interpolation function in Matlab did introduce even worse errors, rendering negative prices for S close to the strike.

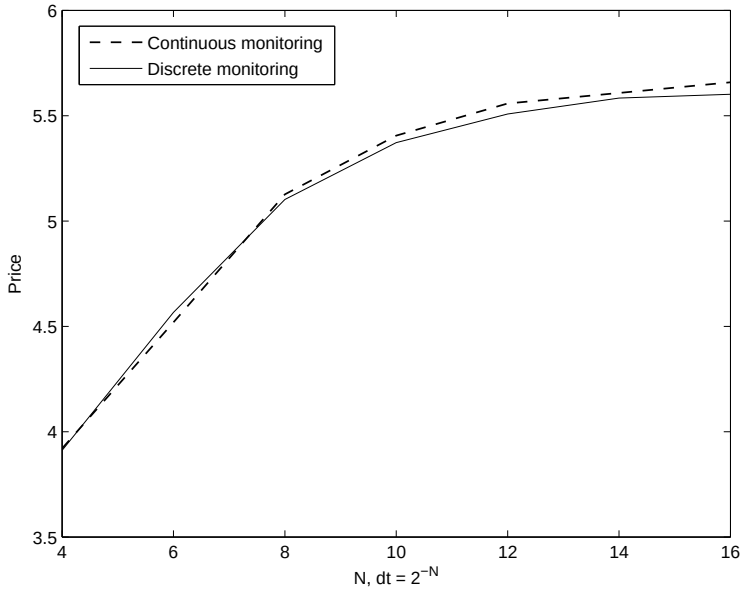

Figure 3.8: Price convergence of up-and-out call

3.5 Barrier Options

In this section we focus on pricing of the up-and-out barrier option in the Heston model. The calculations are done using Monte Carlo simulation. As mentioned previously, a European up-and-out barrier option pays out like a ordinary call option if the asset price stays below a specified boundary, and zero if the price hits or crosses this boundary.

3.5.1 Pricing

To assess the importance of high-resolution paths in the Monte Carlo computations, as well as to indicate whether such a scheme converges to a fixed price, a range of prices have been computed, using paths of increasing resolution. In Figure 3.8, the prices using nonadjusted running extremes as well as adjusted prices (as described in Section 1.5.6) are shown.

3.5.2 Sensitivity analysis

Correlation

To assess the effects of the correlation between the noise processes driving the volatility and the asset path on the barrier option price, we compute the prices on a correlation×strikeprice-grid of the form $\{-0.9, -0.8, \ldots, 0.9\} \times$

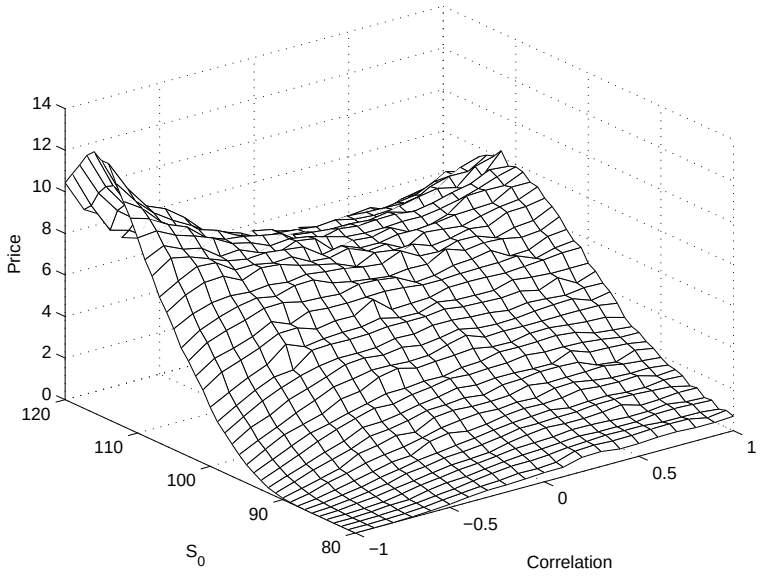

Figure 3.9: Correlation sensitivity surface

$\{80, 81, \ldots, 110\}$. The parameters used are

$$\begin{aligned} S_0 &= 100, \\ T &= 1, \\ r &= 0.03588, \\ v_0 &= 0.0082, \\ \theta &= 0.0168, \\ \kappa &= 6.21, \\ \eta &= 0.625 \end{aligned}$$

and the upper boundary is $ub = 130$. Each price was computed using 1000 paths and a path resolution of $\Delta_t = 2^{-13}$. The sensitivity surface is shown in Figure 3.9. We notice that a large negative correlation results in a higher price for initial prices close to the boundary. The explaination for this may be that during volatility spikes, the asset price process falls. This reduces the risk of boundary crossings, therefor leading to a higher price. For lower initial asset prices, positive correlation gives an upward force on the trajectory, increasing the payoff at maturity, while distanced from the boundary.

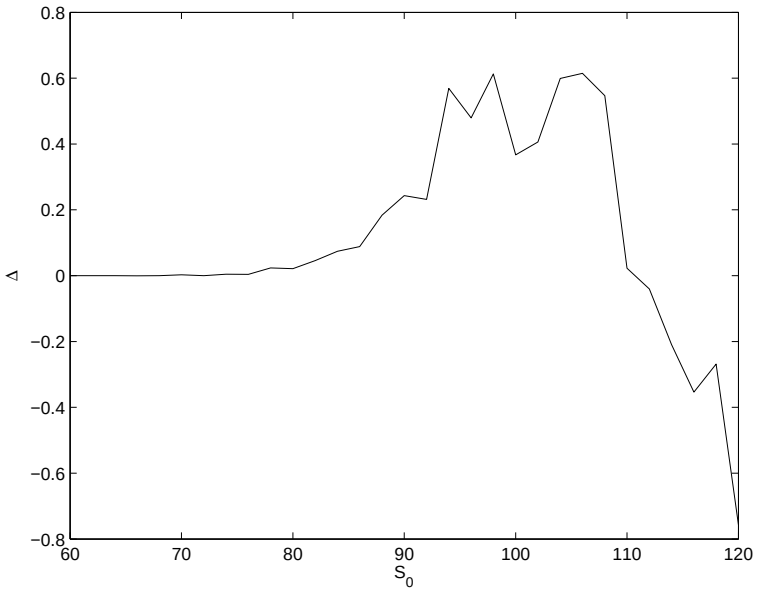

Figure 3.10: Delta versus initial asset price for up-and-out call

Greeks

The Greeks are computed using Monte Carlo and a finite difference approach. The path resolution used in all calculations is $\Delta_t = 2^{-10}$ and the number of trajectories used is 500000. Ideally, a higher resolution would be desirable, but the computational burden becomes overwhelming because of the many paths needed. The Delta shown below took a little more than twelve hours to compute on an Apple iBook G4 with 1.25 GHz processor speed.

Delta For the Delta, $\Delta = \frac{\partial C(\cdot)}{\partial s_0}$, we compute the sensitivity for the s_0-range $\{60, 62, \ldots, 120\}$, using a difference step of $\Delta_{s_0} = 0.1$. Because of the high variability of the Monte Carlo prices, the resulting calculation is not very smooth. As the initial price starts to increase towards the barrier, the delta rises, but for values close to the barrier it falls and eventually becomes negative, as seen in Figure 3.10.

3.6 Lookback Options

In this section we look at pricing of a type of lookback option called the maximum-to-date call option (as introduced in Section 1.2.1). This option

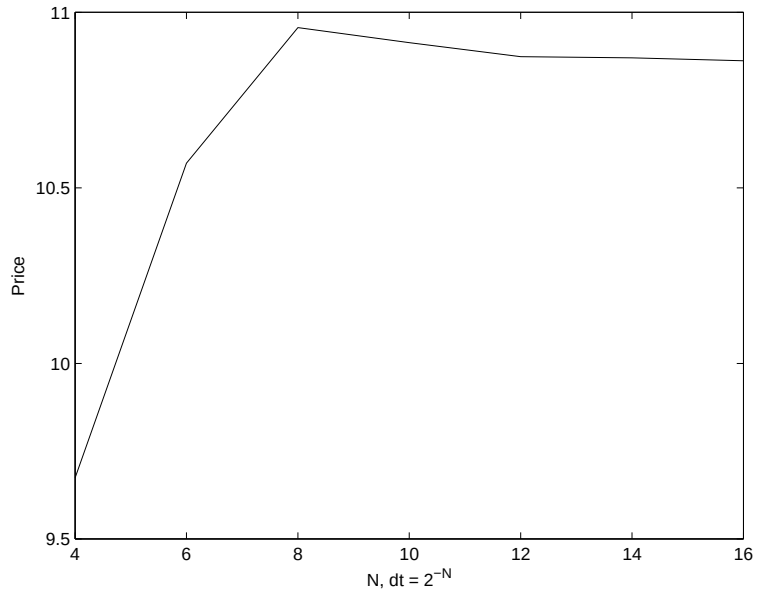

Figure 3.11: Price convergence of a maximum-to-date call option

is similar to the call option, with the difference that the strike is compared to the maximum of the asset price during the life of the option, as opposed to only looking at the ending price as in the ordinary call case.

3.6.1 Pricing

The pricing of lookback options are similar to that of the barrier option case. We show the convergence of the price as resolution increases. This is shown in Figure 3.11.

3.6.2 Sensitivity Analysis

Correlation

That the price of the maximum-to-date call option increases with positive correlation is clear since it provides upward force. The effect is pronounced for S_0 at- or in-the-money. See Figure 3.12.

3.7 Asian options

In this section we look at pricing results on arithmetic Asian call options (as introduced in Section 1.2.1). Asian options are options on the mean

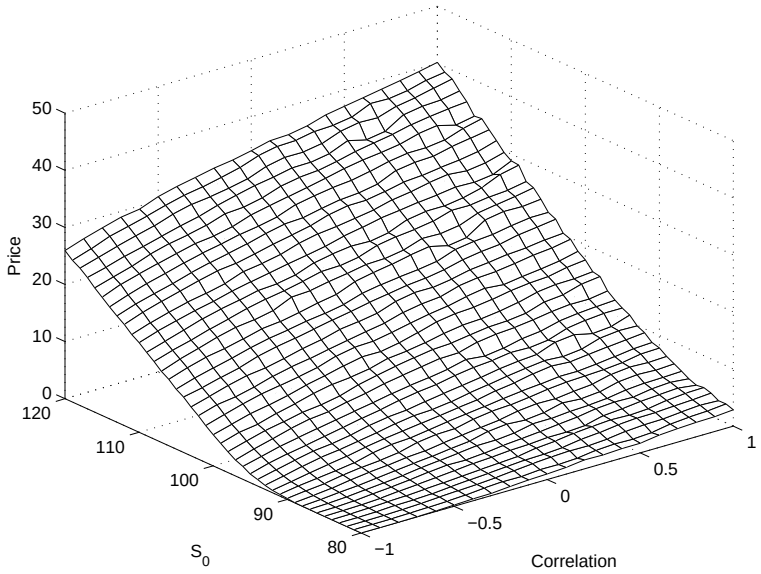

Figure 3.12: Correlation sensitivity surface for maximum-to-date call option

of the stock price, and the payoff of the Asian call options is $V(t) = (\frac{1}{t-a}\int_a^t S(s)ds - K)^+$ where a denotes the point in time from where the mean is taken. We chose to set $a = 0$, hence the mean is taken over the entire lifetime of the option.

3.7.1 Pricing

The Monte Carlo method for these types of options is straightforward and the pricing results are promising. In Figure 3.13 we can see that for low resolutions of the asset paths, we get an upward effects, but that the price narrows in to a common value as the paths get more and more refined.

3.7.2 Sensitivity analysis

Correlation

The correlation surface for the asian call is considerable more flat compared to the barrier type of options. The surface is shown in Figure 3.14. The price of the option rises almost linearly with increased correlation. A positive correlation will give an upward effect on the asset path, increasing the mean. This in turn increase the payoff at maturity.

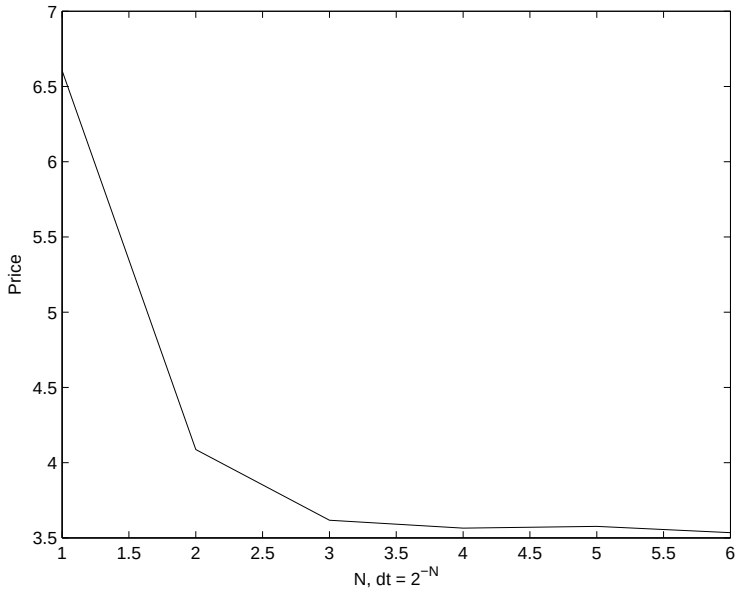

Figure 3.13: Price convergence of arithmetic asian call

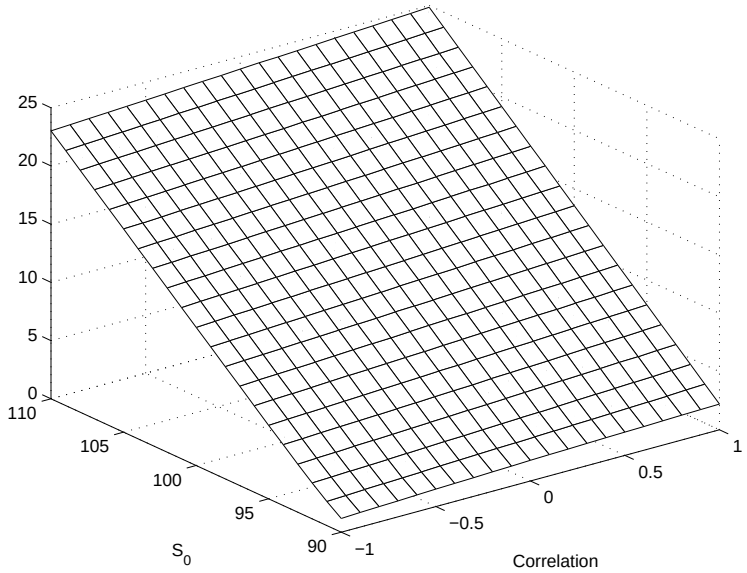

Figure 3.14: Correlation surface of arithmetic asian call

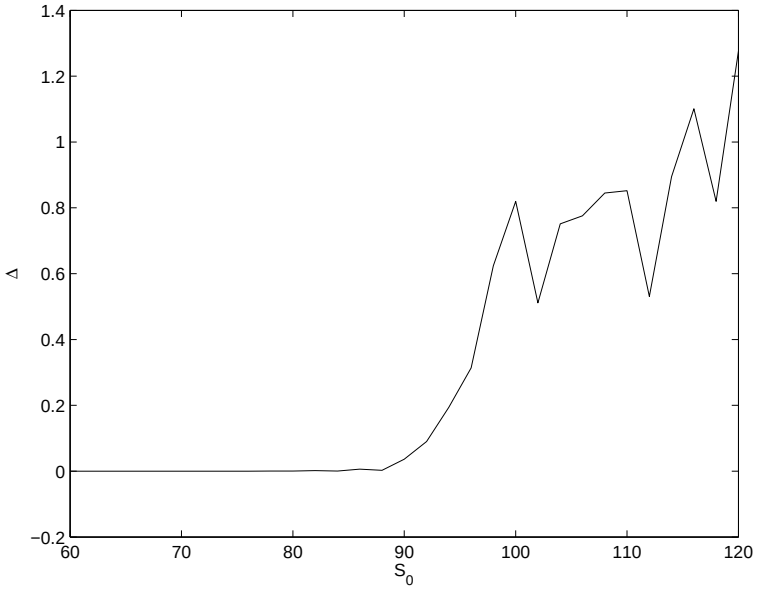

Figure 3.15: Delta versus initial asset price for arithmetic asian call

Greeks

As for the barrier options, the greeks are too computationally burdensome to compute using Monte Carlo. Here we present merely the Delta. It is shown in Figure 3.15.

Chapter 4

Conclusions

What conclusion may then be drawn from the simulations made in this thesis? First of all we may conclude that the Black-Scholes market model does not give a good description of actual market behavior. The assumption of constant volatility is very much an oversimplification, raising effects such as implied volatility smiles. The Heston framework provide remedy for this, and allows for market shaped smiles as empirically shown in the thesis.

When it comes to derivative pricing, it became clear that the Monte Carlo approach was the most accessible, and we did not succeed in implementing neither a working PDE-solver nor a lattice-based solver. The PDE method did unfortunately lead to instabilities, and the lattices produced flawed prices.

The Monte Carlo method wasn't without deficiencies either. Because of the discrete setting, the approximate solution of the volatility SDE tended to become negative from time to time. This made the whole method break down since the asset volatility then became comlex. Our modification to the numerical method in order to avoid this behavior seems to have introduced a bias in the pricing. It is also apparent that we need a very high path resolution in order to correctly price the options. This makes the method computationally demanding.

Since we cannot compare the prices of the path dependent option with analytical prices, we can only infer that the Monte Carlo method converge to a fixed price with increased resolution. Whether this price is different from a theoretical could not be assessed, but the bias apparent in the pricing of the European calls casts doubts on the validity of the Monte Carlo prices for the path dependent options as well.

Bibliography

[1] Ait-Sahalia, Y., Kimmel, R.,
'Maximum Likelihood Estimation of Stochastic Volatility Models',
Working paper, Princeton University, 2005

[2] Bates, D.,
'Jumps and Stochastic Volatility: Exchange Rate Processes Implicit in Deutsche Mark Options',
The Review of Financial Studies **9**, 69-107, 1996

[3] Black, F., Scholes, M.,
'The pricing of options and corporate liabilities',
Journal of Political Economy **81**, 637-654, 1973

[4] Brodie, M., Kaya, Ö.,
'Exact Simulation of Stochastic Volatility and other Affine Jump Diffusion Processes',
Working paper, Columbia University, 2004

[5] Byström, H.,
'Stochastic Volatility and Pricing Bias in the Swedish OMX-Index Call Option Market',
Working paper, Lund University, 2000

[6] Chesney, M., Scott, L.,
'Pricing European Currency Options: A Comparison of the Modified Black-Scholes Model and a Random Variance Model'
The Journal of Financial and Quantitative Analysis **24**, 267-284, 1989

[7] Cox, J., Ingersoll, J., Ross, S.,
'A Theory of the Term Structure of Interest Rates',
Econometrica **53**, 385-408, 1985

[8] Duffie, D., Singelton, K. Pan, J.,
'Transform Analysis and Asset Pricing for Affine Jump-Diffusions',
Econometrica **68**, 1343-1376, 2000

[9] Glasserman, P.,
'Monte Carlo Methods in Financial Engineering',
Springer Verlag, 2003

[10] Guan, K., L., Xiaoqiang, G.,
'Pricing American Options with Stochastic Volatility: Evidence from the S&P 500 Futures Options',
The Journal of futures Markets **20**, 625–659, 2000

[11] Heston, S.,
'A Closed-Form Solution for Options with Stochastic Volatility with Application to Bond and Currency Options',
The Review of Financial Studies **6**, 327-343, 1993

[12] Hull, J., White, A.,
'The Pricing of Options on Assets with Stochastic Volatilities',
The Journal of Finance **42**, 281-300, 1987

[13] Merton, R.,
'Option pricing when underlying stock returns are discontinuous',
Journal of Financial Economics **3**, 125-144, 1976

[14] Mikhailov, S., Nögel, U.,
'Heston's Stochastic Volaility Model Implementation, Calibration and Some Extensions',
Wilmott Magazine, 2005

[15] Rebonato, R.,
'Volatility and Correlation', Second edition,
Wiley, 2004

[16] Scott, L.,
'Option Pricing when the Variance Changes Randomly: Theory, Estimation, and an Application',
The Journal of Financial and Quantitative Analysis **22**, 419-438, 1987

[17] Stein, E., Stein J.,
'Stock Price Distributions with Stochastic Volatility: An Analytic Approach',
The Review of Financial Studies **4**, 727-752, 1991